

# Development and application of rotationally compensated RARE

A.J. Sederman, K.G. Hollingsworth, M.L. Johns\*, L.F. Gladden

*Department of Chemical Engineering, University of Cambridge, Pembroke Street, CB2 3RA, UK*

Received 23 April 2004; revised 28 June 2004

Available online 12 September 2004

---

## Abstract

In this paper we describe a new extension to the RARE rapid imaging technique—ROTACOR—which compensates for constant sample rotational motion by rotating the direction of the gradient coordinate system (read and phase directions) between each refocusing RF pulse and therefore between each acquisition of a line of  $k$ -space in the read direction. In the laboratory frame this corresponds to an irregularly sampled  $k$ -space raster; for a sample rotating at the predefined rotation rate this will correspond to the sampling of a rectilinear  $k$ -space raster. This technique is applied to two rotating systems. First, to demonstrate the technique, a rotating mixing paddle in water is imaged using conventional RARE and then using the ROTACOR sequence, demonstrating the improvement of image quality produced by ROTACOR. Second, ROTACOR is used to image the deformation of water droplets in silicone oil, being sheared in a wide-gap Couette cell. Accurate imaging of the droplet shape as a function of shear rate, permits determination of the interfacial tension between the two fluids concerned; the results compare favourably with reported literature values.

© 2004 Elsevier Inc. All rights reserved.

**Keywords:** RARE; Rapid imaging; Rotation; Interfacial tension

---

## 1. Introduction

The rapid acquisition with relaxation enhancement (RARE) pulse sequence was first introduced by Hennig et al. [1], as a fast method for the acquisition of clinical magnetic resonance (MR) images. RARE allows a complete 2D image to be captured using a single radio-frequency excitation, reducing the imaging time required from an order of minutes with conventional imaging to less than one second. The sequence has found applications in both medical and non-medical MRI, e.g. [2,3].

Nevertheless the acquisition of quantitative images of dynamic systems still requires a spatially constant geometry over the image acquisition time. There have been several attempts to correct for artefacts, due to motion during the image acquisition, based on post-processing of the acquired data, e.g. [4–6]. An ability to acquire

artefact-free images of rotating objects provides the opportunity to study appropriate dynamic systems, when even using standard fast imaging techniques the images would be blurred. A modification to RARE is presented here which compensates for the rotation of the sample being imaged during the image acquisition time—ROTationally COMPensated RARE (ROTACOR). This is demonstrated on a paddle rotating in a tube of water and on droplets of water in silicone oil, being sheared inside a wide-gapped Couette cell. A Couette cell is two concentric cylinders with the larger cylinder static, the smaller cylinder placed inside the large cylinder and rotated at a known rotational velocity and fluid in the gap between the cylinders. When the gap between the cylinders is wide, as used here, the shear rate of the fluid is a function of radial position. The accurate measurement of droplet shape deformation, only possible due to the application of ROTACOR, as a function of shear rate is then used to estimate the interfacial tension between the two respective fluids.

---

\* Corresponding author. Fax: +44 1223 334796.

E-mail address: [mlj21@cheng.cam.ac.uk](mailto:mlj21@cheng.cam.ac.uk) (M.L. Johns).

## 2. Background

### 2.1. Description of ROTACOR pulse sequence

If a normal RARE sequence is used on a rotating system, significant distortions in the image will occur at high-rotational speeds due to motion over the total acquisition timescale of the image (typically 384 ms for a  $128 \times 128$  image). A novel RARE sequence, ROTACOR as shown in Fig. 1A, has been developed which is able to compensate for the rotational movement of a body during image acquisition. This works by reorienting the direction of the imaging gradients between each cycle or echo acquisition, as shown schematically in Fig. 1B, to ensure that the  $k$ -space raster remains aligned with a chosen rotational velocity,  $\omega$ . This means that the directions of the read and phase gradients rotate after each cycle or echo acquisition, but remain perpendicular to one another, their angle with the  $x$ -axis being noted as  $\alpha$  and  $\alpha + \pi/2$ , respectively.  $\alpha$  increases with  $t$ , the time between successive echo acquisitions, by an amount  $\omega t$ . Fig. 1B shows two typical orientations of  $k$ -space. Our use of rotating magnetic gradients to acquire rapid images of rotating objects bears some resemblance to the use of rotating gradients along with MAS [7] to acquire solid-state images using linear back projection methods.

In experiments performed in our work, ( $\omega < 2$  rev/s), the rotational movement between unwind and rewind phase gradients ( $\sim 1.5$  ms duration) is not significant, however for higher rotational velocities, it would be necessary to reorient the read and phase gradients before and after the acquisition, and at even larger angular velocities the read gradient orientation during acquisition. Note that unlike conventional RARE or UFLARE methods [8], the sequence begins and ends at the origin of  $k$ -space between each cycle or echo acquisition. This increases the robustness of the pulse sequence since the origin of  $k$ -space is the only point unaffected by the gradient rotation. Practically RARE involves the acquisition of both spin and stimulated echoes; these must all complete the cycle at the same point in  $k$ -space, which is ensured by the return to the origin of  $k$ -space after each cycle. Homospoil gradients around each RF refocusing pulse (Fig. 1A) are consequently applied in the slice direction such that any FID generated by the refocusing pulses will be dephased and thus to avoid any SSFP contribution. To achieve the successful implementation of ROTACOR, the following conditions must be met:

- (i) The centre of rotation of the object being imaged and the centre of the imaging gradients must coincide.

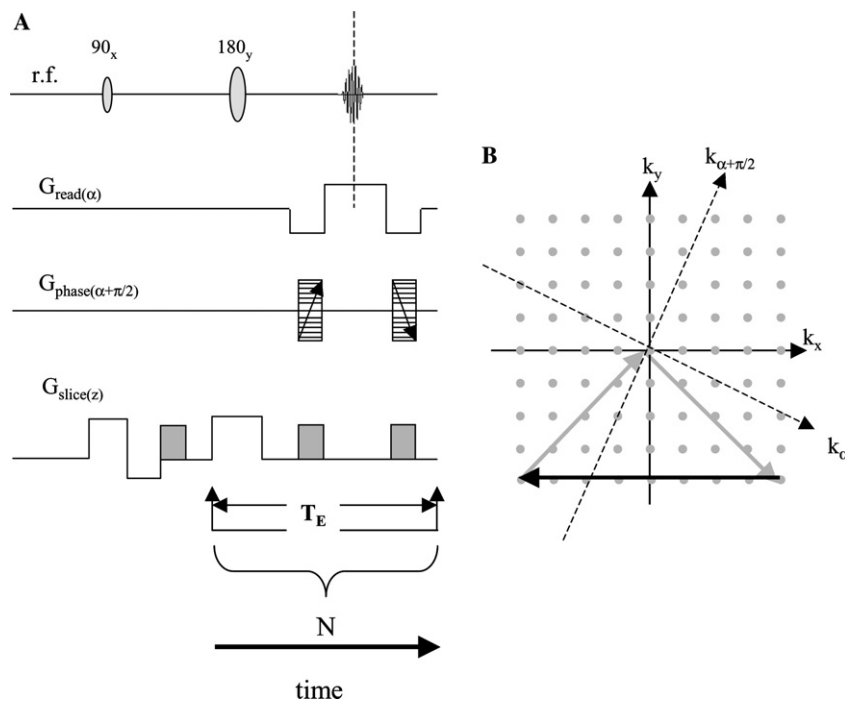


Fig. 1. (A) The ROTACOR pulse sequence as described in the text and (B) the associated  $k$ -space raster. The pulse sequence is a variant of the RARE pulse sequence with the read and phase directions rotated with respect to the laboratory-frame after each echo acquisition such that the orientation of  $k$ -space relative to the rotating object remains constant. After each echo acquisition, the system is returned to the centre of  $k$ -space, which is not affected by sample rotation. Consequently homospoil gradients (shown in grey) are applied in the slice direction on either side of the refocusing  $180^\circ$  pulse. The direction of the read and phase gradients ( $\alpha, \alpha + \pi/2$ ) are rotated by  $\omega \cdot T_E \cdot 2\pi$  after each refocusing pulse, where  $\omega$  is the rotation frequency.

- (ii) The angular velocity,  $\omega$ , of the object to be imaged and of the  $k$ -space raster must be matched. This is considered further in the next section.

## 2.2. Determination of an appropriate $\omega$

For a solid object, all parts of the rotating object have the same angular velocity,  $\omega$ , and hence it is easily possible to compensate for the rotation of such an object. However, in the case of a droplet suspended in another fluid, being sheared in a wide-gap Couette cell, there will be a distribution of rotational velocities dependent upon radial position. The silicone oils used in our study have Newtonian rheology and a no-slip condition is preserved at the outer and inner walls of the Couette. Therefore, the velocity of the fluid falls off from a maximum next to the inside wall of the Couette to zero at the outer wall of the Couette.

To compensate properly for a droplet rotating in the Couette, it is therefore necessary to determine its radial position. This is possible as a droplet being sheared in a Couette will migrate from its original radial position to an equilibrium radial position in the Couette [9]. This equilibrium position depends on the geometry of the Couette and the size of the droplet in question. In a narrow-gap Couette the equilibrium position lies approximately equidistant from each wall; in a wider-gap Couette the equilibrium position is shifted towards the inside wall of the Couette [10]. In this work the droplet is allowed to attain its equilibrium position before imaging takes place. Since we know the rheology of the silicone oil to be Newtonian, we are able to calculate both the velocity,  $v_\phi$ , and shear rate,  $\dot{\gamma}$ , at the equilibrium position of the droplet, by the following formulae [11]:

$$v_\phi = \Omega r_i \frac{R(1 - R^{-2})}{K(1 - K^{-2})} \quad (1)$$

and

$$\dot{\gamma} = \frac{2\Omega R^{-2}}{1 - K^{-2}}, \quad (2)$$

where  $R = r_{eq}/r_o$ ,  $K = r_i/r_o$ ,  $r_i$  is the outer radius of the inner tube,  $r_o$  is the inner radius of the outer tube,  $r_{eq}$  is the equilibrium radial position of the droplet, and  $\Omega$  is the angular velocity of the inner cylinder. The angular velocity of the deformed droplet,  $\omega$ , is thus given by

$$\omega = \frac{v_\phi}{r_{eq}}. \quad (3)$$

The rotational compensation used in ROTACOR, when applied to droplets being sheared, is thus determined according to the angular velocity,  $\omega$ , calculated using Eqs. (1) and (3). This approach was checked by performing multiple image acquisitions with ROTA-

COR at various values of  $\omega$ , these showed that the sharpest images were produced for the value of  $\omega$  calculated using Eqs. (1) and (3).

## 2.3. Interfacial tension measurement

It has long been observed that a droplet in a simple shear field will deform. The first treatment of the theory and experimental results for droplet deformation in pure shear flow and plane hyperbolic flow was given by Taylor [11], using a force balance between the normal stresses that act on the droplet and the capillary pressure that results from the deformation of the droplet. Taylor showed the deformation experienced by the sheared droplet was proportional to the capillary number of the emulsion system multiplied by a factor determined by the viscosity ratio of the system

$$\frac{L - B}{L + B} = D = Ca \cdot \frac{19\kappa + 16}{16\kappa + 16}, \quad (4)$$

where  $L$  and  $B$  are the length and breadth of the droplet, respectively,  $D$  is the deformation of the droplet,  $\kappa$  is the ratio of the viscosity of the droplet phase to the continuous phase, and  $Ca$  is the capillary number

$$Ca = \frac{\eta_c \dot{\gamma} a}{\sigma}, \quad (5)$$

where  $\eta_c$  is the viscosity of the continuous phase,  $\dot{\gamma}$  is the shear rate,  $a$  is the radius of the un-deformed droplet, and  $\sigma$  is the interfacial tension between the droplet and the continuous phase.

## 2.4. Experimental

All images were acquired using a Bruker DMX 300 spectrometer with a magnetic field strength of 7.07 T corresponding to a  $^1\text{H}$  resonance frequency of 300 MHz. A 25 mm inner-diameter bird-cage RF coil was used. The rotating gradient wave forms are generated with in-house software (IDA) using a sine/cosine modulation in the  $x$  and  $y$  gradient directions for both the read and phase gradients. A wide-gap Couette cell consisting of two concentric glass tubes was positioned inside the RF coil. The inner tube had an outer radius of 2.5 mm (and was filled with water) and the outer tube had an inner radius of 8.8 mm. For the preliminary experiments, the inner glass tube was replaced by a single-blade nylon paddle with a rectangular cross-section of  $5.9 \times 1.9$  mm. The inner tube or the nylon paddle was rotated by a drive shaft attached to an overhead motor positioned outside the magnet, whilst the outer tube was fixed in position. When imaging sheared droplets, the fluids were positioned in the annulus between the tubes of the wide-gap Couette.

Silicone oil (dimethylpolysiloxane) of viscosity 1000 or 12,500 cSt (supplied by Sigma–Aldrich, UK) was

used as the continuous phase when imaging the sheared droplets, which were composed of either water or water containing the non-ionic surfactant, Tween 60 (supplied by Sigma–Aldrich, UK) at a concentration of 1 wt%. Such surfactant-containing droplets will deform more readily due to the presence of the surfactant and the consequential lowering of the interfacial tension. An Eppendorf Multipette Plus was used to produce either 1 or 2  $\mu\text{L}$  water droplets (corresponding to an un-deformed radius of 0.62 or 0.78 mm, respectively) in the silicone oil. Contrast between the silicone oil and the water phases was realised by either:

- (i) Paramagnetic addition. Adding  $\text{MnSO}_4$  to the water at a concentration of 0.005 M, consequently reducing the  $T_2$  of the water to approximately 1 ms and effectively eliminating water signal from the RARE images. The rheology of the water was unaffected by this addition.
- (ii) Inversion recovery. Nulling out the signal from the oil using a compound  $180^\circ$  pulse prior to the ROTACOR pulse sequence. These were separated by a time period of  $0.6931 \times T_1$  (silicone oil). This nulled out the signal from the silicone oil ( $T_1 = 1.27$  s) but retained the signal from the water in the droplets ( $T_1 = 2.89$  s).

### 3. Results and discussion

#### 3.1. Rotational compensation of a rotating solid body

RARE images of a solid nylon paddle were taken whilst it was rotating at a speed,  $\omega$ , of 1.6 rev/s. Application of conventional RARE resulted in the image shown in Fig. 2A, whilst application of the ROTACOR sequence resulted in the image shown in Fig. 2B. The darker areas (corresponding to signal loss) in the water on either side of the paddle, in both images, are due to the paddle moving water vertically out of the selected slice

during image acquisition, which is hence replaced by water that has not been exposed to the initial RF excitation. The image shown in Fig. 2A displays significant blurring at the outer edges of the paddle. During image acquisition (lasting 192 ms), the paddle would have rotated through 1.93 rad; this is leading to blurring of the image and a mis-registration of the shape of the paddle. The image acquired with ROTACOR (Fig. 2B) is clearly much better defined. The paddle will only rotate 0.03 rad during each cycle or echo acquisition, resulting in a much improved representation of the paddle shape.

#### 3.2. Rotational compensation of sheared droplets

A similar comparison of two ‘pure’ water droplets in 1000 cSt silicone oil, being sheared in a wide-gap Couette cell at a local shear rate,  $\omega$ , of 0.63 rev/s, is shown in Fig. 3A (acquired with conventional RARE) and Fig. 3B (acquired with ROTACOR). Rotational compensation was applied according to the value of  $\omega$  (0.63 rev/s) appropriate for the larger water droplet. Clearly the shape of the larger droplet is more clearly defined when rotational compensation is applied. The smaller droplet was not fully rotationally compensated for, due to its slightly different radial position than the large droplet. Because of this the rotational compensation was 14% too small ( $\omega = 0.72$  rev/s), yet it is clearly visible in the compensated image (Fig. 3B), but is barely visible in the uncompensated image (Fig. 3A—its position is marked with an arrow), its contribution having been blurred over a considerable distance. The relative positions of the two droplets between (A) and (B) has changed because of their different radial positions and hence rotational velocities.

#### 3.3. Estimation of interfacial tension using droplet signal blanking

Figs. 4A–C give examples of images attained of water droplets containing 1% Tween 60 under local droplet shear rates,  $\omega$ , of 0.63, 1.67, and  $3.25 \text{ s}^{-1}$  and using

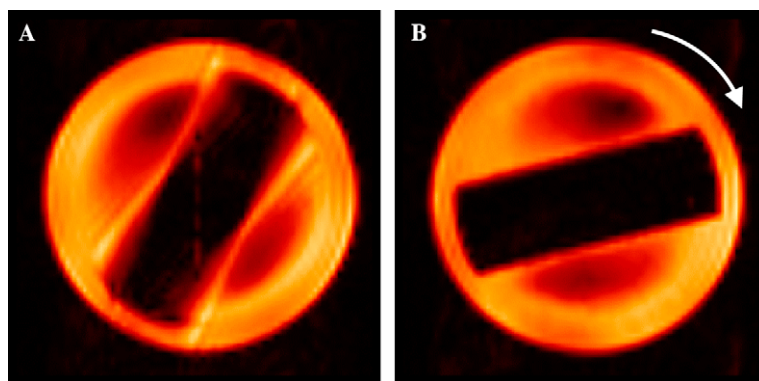


Fig. 2. (A) Conventional RARE and (B) ROTACOR images of a paddle rotating in water at 1.6 rev/s. There is evident blurring of the outer edges of the paddle in (A) but a sharp definition of the paddle shape in (B).

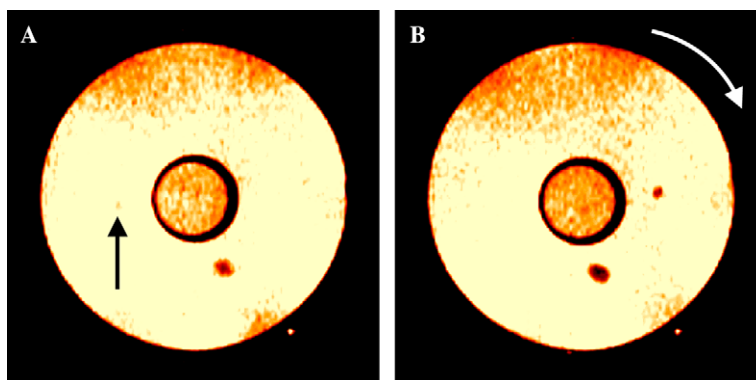


Fig. 3. (A) Conventional RARE and (B) ROTACOR images of two suspended water droplets in 1000 cSt silicone oil. Rotational compensation ( $\omega = 0.62$  rev/s) is appropriate for the larger water droplet. In the RARE image the large droplet is blurred and the small droplet is not seen, whereas the ROTACOR image shows the presence and shape of both water droplets clearly.

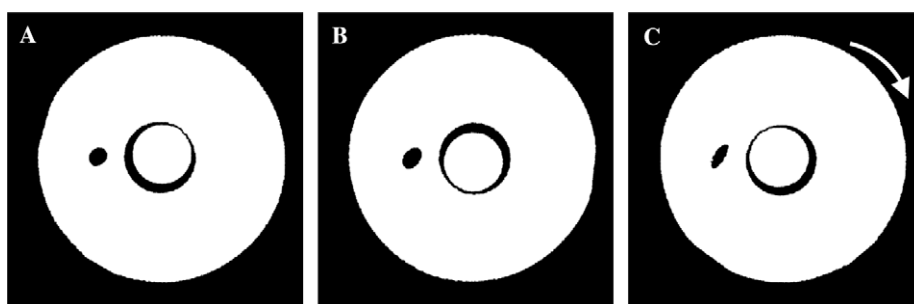


Fig. 4. Images acquired using ROTACOR of 2  $\mu$ L water droplets of 1 wt% Tween 60 with 0.005 M  $\text{MnSO}_4$  in 1000 cSt silicone oil under shear rates of (A)  $0.63 \text{ s}^{-1}$ , (B)  $1.67 \text{ s}^{-1}$ , and (C)  $3.25 \text{ s}^{-1}$ . Water inside the rotating inner cylinder also appears in the images; it is off centre due to its chemical shift relative to that of the silicone oil. The figures have been rotated to show the droplets in the same position in the Couette.

1000 cSt silicone oil as the continuous phase. Extension of the droplets is clearly observed as shear rate is increased. For ease of comparison, the images have been rotated such that the droplets are all at the same position. The main axis of the droplets is inclined at an angle of approximately  $45^\circ$  to the direction of flow, as predicted by theory [11]. By calculating the length of the major axis of the droplet,  $L$ , and the minor axis of the droplet,  $B$ , it is possible to calculate the deformation of the droplet,  $D$ , as a function of local shear rate. A plot of  $D$  versus local shear rate for this particular system is shown in Fig. 5. Applying Eqs. (4) and (5) to the data in Fig. 5, enables the interfacial tension,  $\sigma$ , between the silicone oil and the surfactant containing water to be estimated. The value produced is  $6.1 \text{ mN/m}$ .

Replacing the 1000 cSt silicone oil with 12,500 cSt silicone oil and using inversion recovery to blank out the signal from the silicone oil produced the series of images shown in Figs. 6A–C for water droplets under local droplet shear rates of 0.08, 0.21, and  $0.41 \text{ s}^{-1}$ . The value of  $\sigma$  extracted from this system was  $6.8 \text{ mN/m}$ . These values of  $\sigma$  for both silicone oils compare favourably with a literature value of  $6.6 \text{ mN/m}$  [12], which utilised 5000 cSt silicone oil. Replacing the surfactant-containing water droplets with ‘pure’ water produced a value for  $\sigma$  of

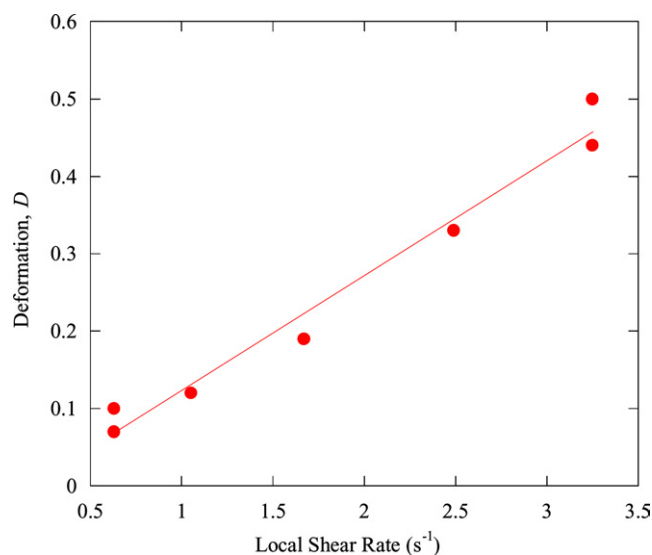


Fig. 5. A plot of droplet shape deformation,  $D$ , versus local shear rate for the droplet imaged in Fig. 4. The solid line represents the best fit of Eqs. (4) and (5) to the experimental data. From the slope it is possible to estimate  $\sigma$ , the interfacial tension between the water (containing 1 wt% Tween 60) and the silicone oil. In this case the value estimated for  $\sigma$  was  $6.1 \text{ mN/m}$ .



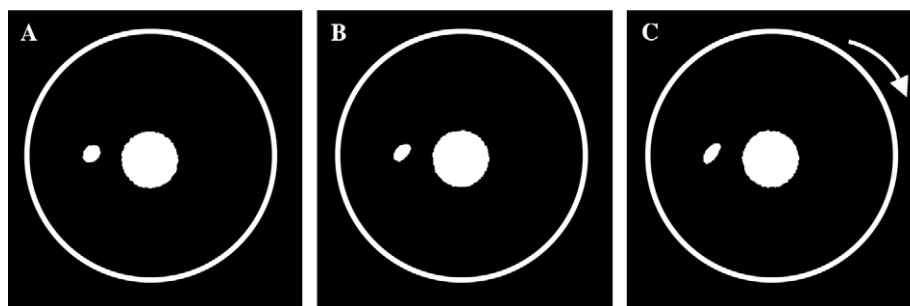


Fig. 6. Images acquired using ROTACOR of 2  $\mu\text{L}$  water droplets containing 1 wt% Tween 60, in 12,500 cSt silicone oil under local shear rates of (A)  $0.08\text{ s}^{-1}$ , (B)  $0.21\text{ s}^{-1}$ , and (C)  $0.41\text{ s}^{-1}$ . Inversion recovery has been used to eliminate the signal from the silicone oil. Water inside the rotating inner cylinder also appears. The figures have been rotated to show the droplet in the same position in the Couette.

34 mN/m for both silicone oils. Clearly the surfactant is reducing the interfacial tension between the water and the silicone oils. This is again in good agreement with literature values of 38 mN/m [13] for distilled water and 45 mN/m for deionised and ultra-filtered water [14].  $\sigma$  is particularly sensitive to impurities in the water [14]. No significant change in  $\sigma$  for 'pure' water droplets with silicone oil viscosity was also observed in [13].

#### 4. Conclusions

It has been shown that rotationally compensated RARE—ROTACOR—allows high-quality imaging of rotating objects. It works by rotating  $k$ -space at the same rotational velocity as the object of interest. This was demonstrated using a rotating nylon paddle, and subsequently applied to droplets being sheared, and hence deformed, in a wide-gap Couette cell. The consequential high-resolution undistorted images of the sheared droplets, as a function of shear rate, enabled the dynamic interfacial tension between the droplet phase and the continuous liquid phase to be estimated. This was performed for a range of systems; results were in good agreement with corresponding literature values. Future work will apply this method to studies of droplet break-up and droplet deformation involving visco-elastic and/or opaque fluids.

#### References

- [1] J. Hennig, A. Nauerth, H. Friedburg, RARE imaging—a fast imaging method for clinical MR, *Magn. Reson. Med.* 3 (1986) 823.
- [2] M.M. Maher, T.A.S. Prosd, J.M. Fitzpatrick, et al., Spinal dysraphism at MR urography: initial experience, *Radiology* 216 (2000) 237.
- [3] L.F. Gladden, M.H.M. Lim, M.D. Mantle, A.J. Sederman, E.H. Stitt, Visualisation of two-phase flow in structured supports and trickle-bed reactors, *Catalysis Today* 79–80 (2003) 203.
- [4] C.A. Wheeler-Kingshott, Y. Cremillieux, S.J. Doran, Burst imaging: rotation artifacts and how to correct them, *J. Magn. Reson.* 143 (2000) 161.
- [5] M.E. Bourgeois, F. Wajer, M. Roth, A. Briguet, M. Decors, D. van Ormondt, C. Segebarth, D. Graveron-Demilly, Retrospective intra-scan motion correction, *J. Magn. Reson.* 163 (2003) 277.
- [6] E.B. Welch, A. Manduca, R.C. Grimm, H.A. Ward, C.R. Jack, Spherical navigator echoes for full 3D rigid body motion measurement in MRI, *Magn. Reson. Med.* 47 (2002) 32.
- [7] D.G. Cory, A.M. Reichwein, J.W.M. van Os, W.S. Veeman, NMR images of rigid solids, *Chem. Phys. Lett.* 143 (1988) 467.
- [8] D.G. Norris, Ultrafast Low-Angle Rare—U-Flare, *Magn. Reson. Med.* 17 (1991) 539.
- [9] P.C.H. Chan, L.G. Leal, An experimental study of drop migration in shear flow between concentric cylinders, *Int. J. Multiphase Flow* 7 (1981) 83.
- [10] J.M. McKelvey, *Polymer Processing*, Wiley, New York, 1962, p. 106.
- [11] G.I. Taylor, The formation of emulsions in definable fields of flow, *Proc. R. Soc. (London)* 146A (1934) 501.
- [12] F.D. Rumscheidt, S.G. Mason, Particle motions in sheared suspensions: deformation and burst of fluid drops in shear and hyperbolic flow, *J. Colloid Interface Sci.* 16 (1961) 238.
- [13] C.Y. Wang, R.V. Calabrese, Drop breakup in turbulent stirred-tank reactors: relative influence of viscosity and interfacial tension, *AIChE J.* 32 (1986) 667.
- [14] G. Zhou, S.M. Kresta, Evolution of drop size distribution in liquid–liquid dispersions for various impellers, *Chem. Eng. Sci.* 53 (1998) 2099.